

Preparation and Antiproliferative Activity Evaluation of Juglone-Loaded BSA Nanoparticles

Ali Jahanban-Esfahlan¹, Soodabeh Davaran^{2,3}, Siavoush Dastmalchi^{1,2,4*}

¹Biotechnology Research Center, Tabriz University of Medical Sciences, Tabriz, Iran.

²School of Pharmacy, Tabriz University of Medical Sciences, Tabriz, Iran.

³Drug Applied Research Center, Tabriz University of Medical Sciences, Tabriz, Iran.

⁴Faculty of Pharmacy, Near East University, POBOX: 99138, Nicosia, North Cyprus, Mersin 10, Turkey.

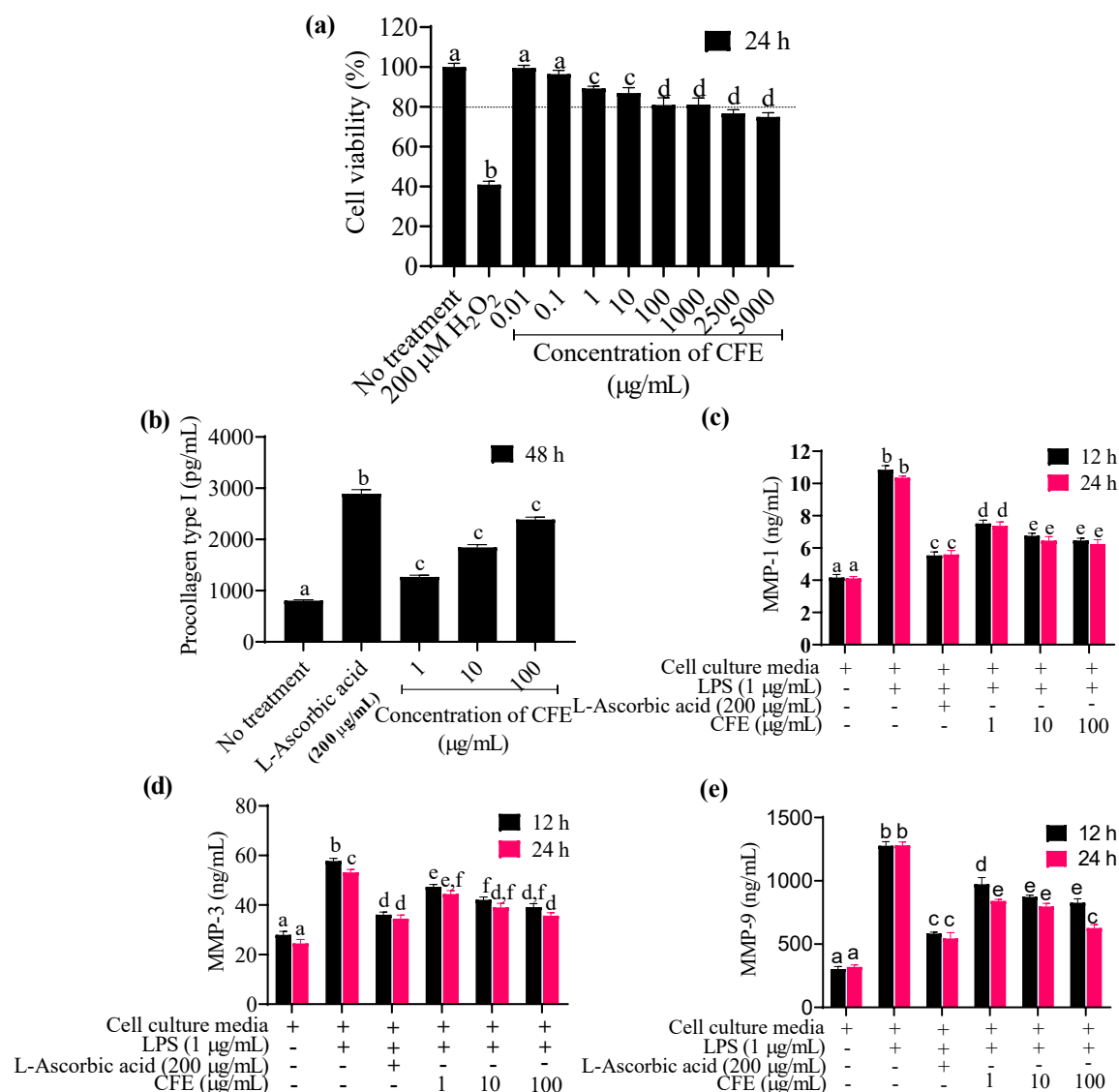


Figure S1. Cytotoxic and biological properties of CFE for cosmetic applications: (a) cytotoxicity to HDFn cells, (b) procollagen type I synthesis, (c) inhibitory activity of CFE against MMP-1, (d) inhibitory activity of CFE against MMP-3, and (e) inhibitory activity of CFE against MMP-9. Values sharing the same letter above the bars indicate a lack of significant difference ($p > 0.05$).

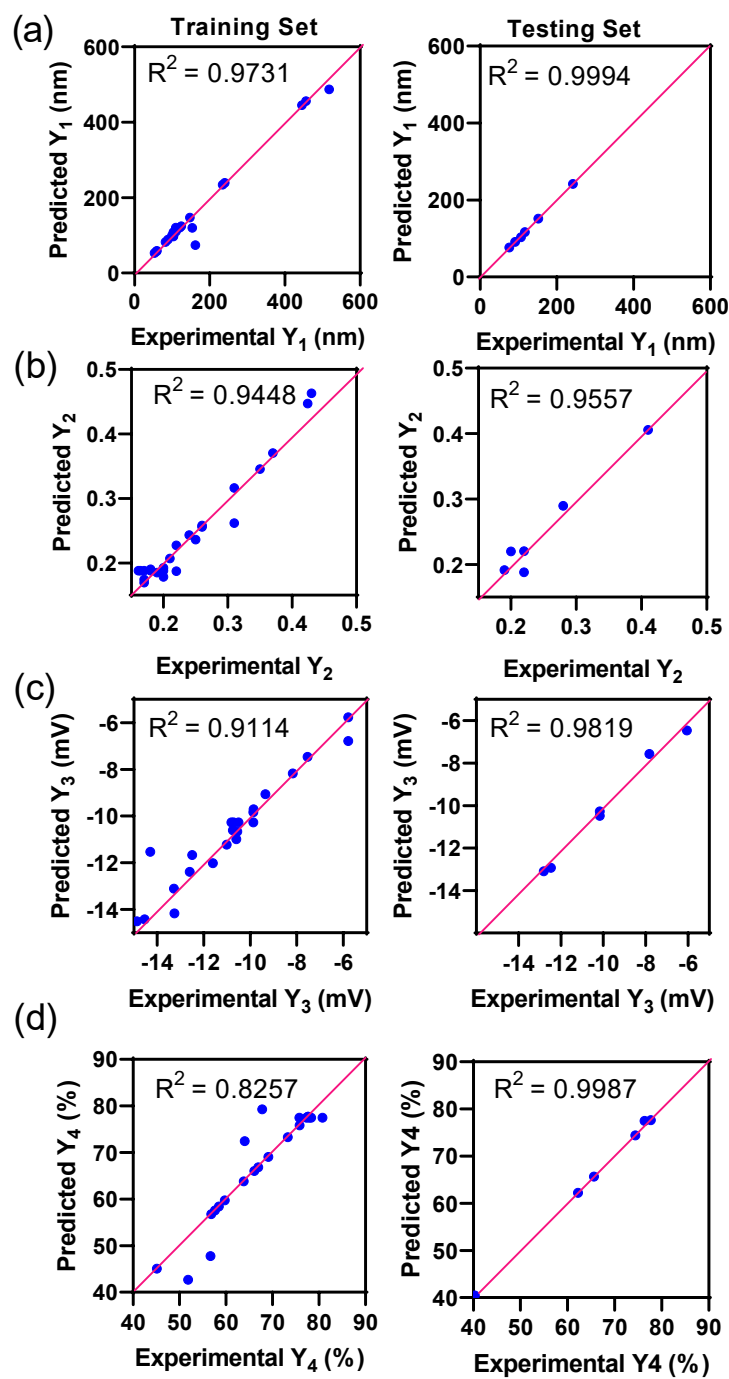


Figure S2. Plots showing the relationship between experimental and predicted values in the training (left panel) and validation sets (right panel): (a) hydrodynamic diameter; (b) PDI; (c) zeta potential; and (d) EE% of 5CQA in NLCs.

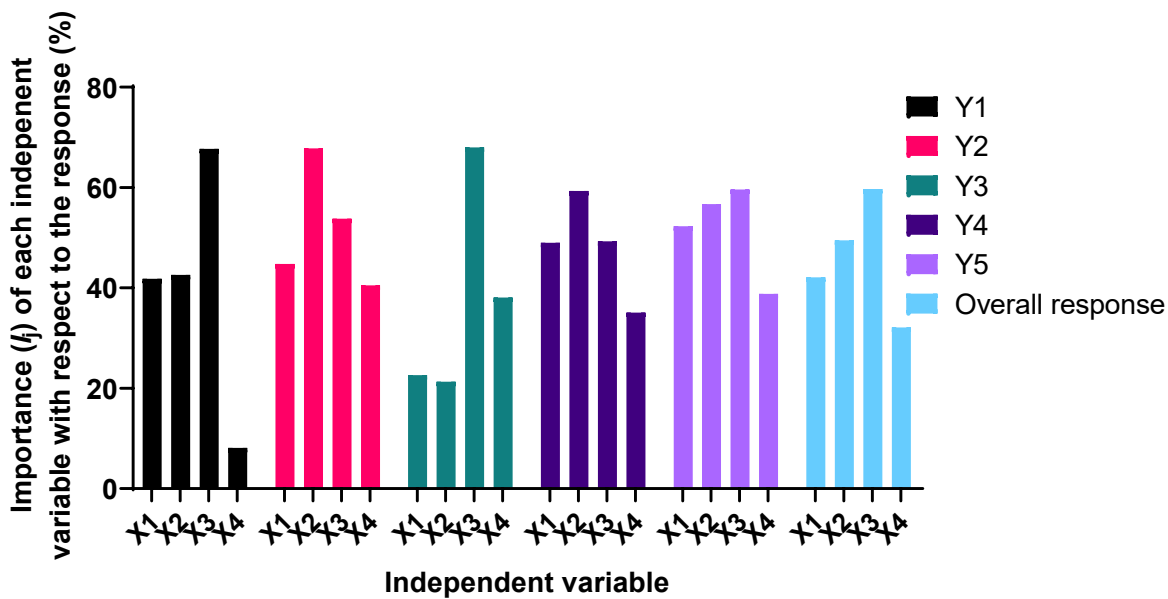


Figure S3. Plots showing the I_j value of each independent variable with respect to the responses.

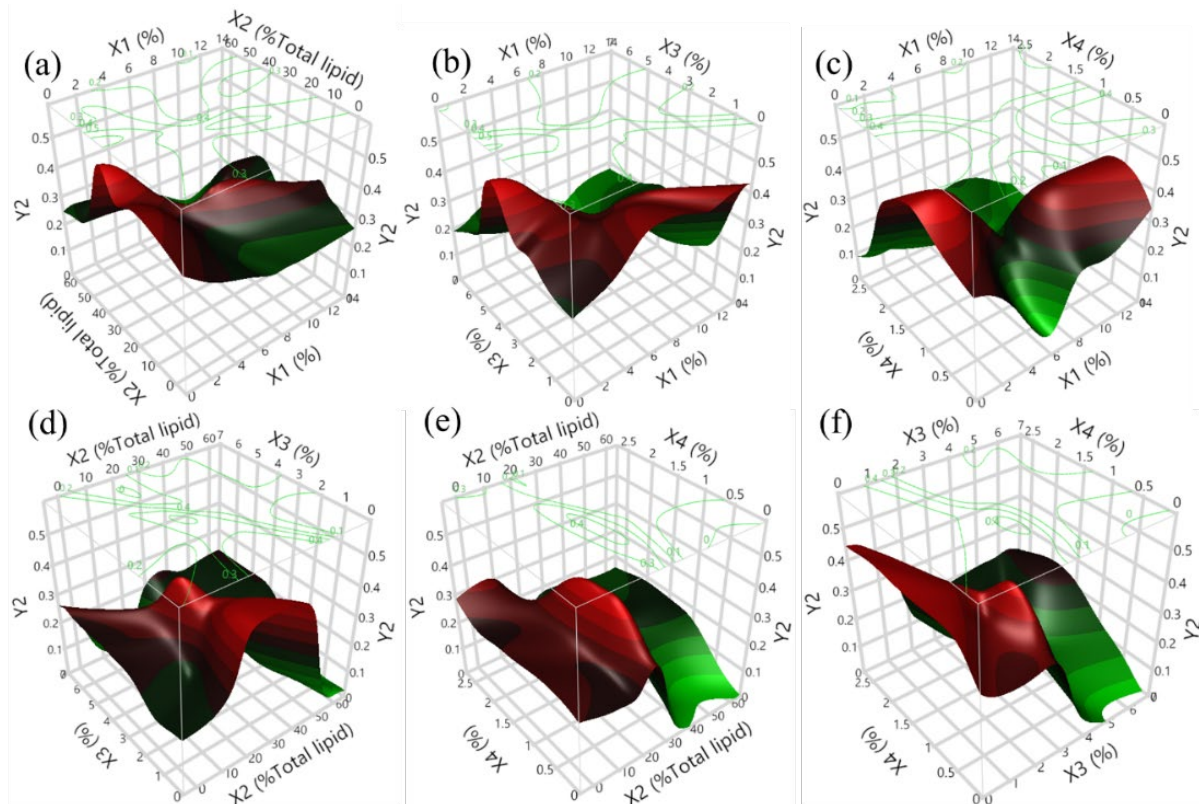


Figure S4. 3D plots showing the combined effects of independent variables on the PDI of CFE-NLCs (refer to Table 1 for X_1 – X_4 and Y_2).

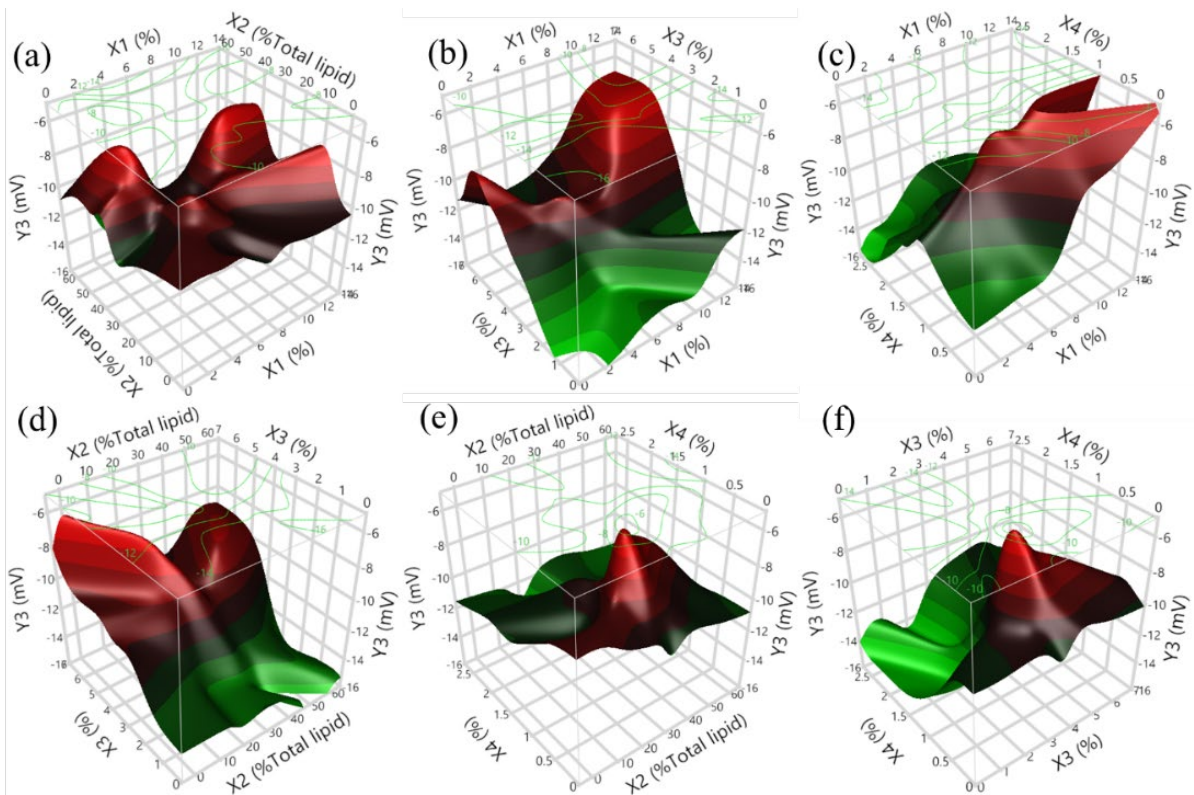


Figure S5. 3D plots showing the combined effects of independent variables on the zeta potential of CFE-NLCs (refer to Table 1 for X_1 - X_4 and Y_3).

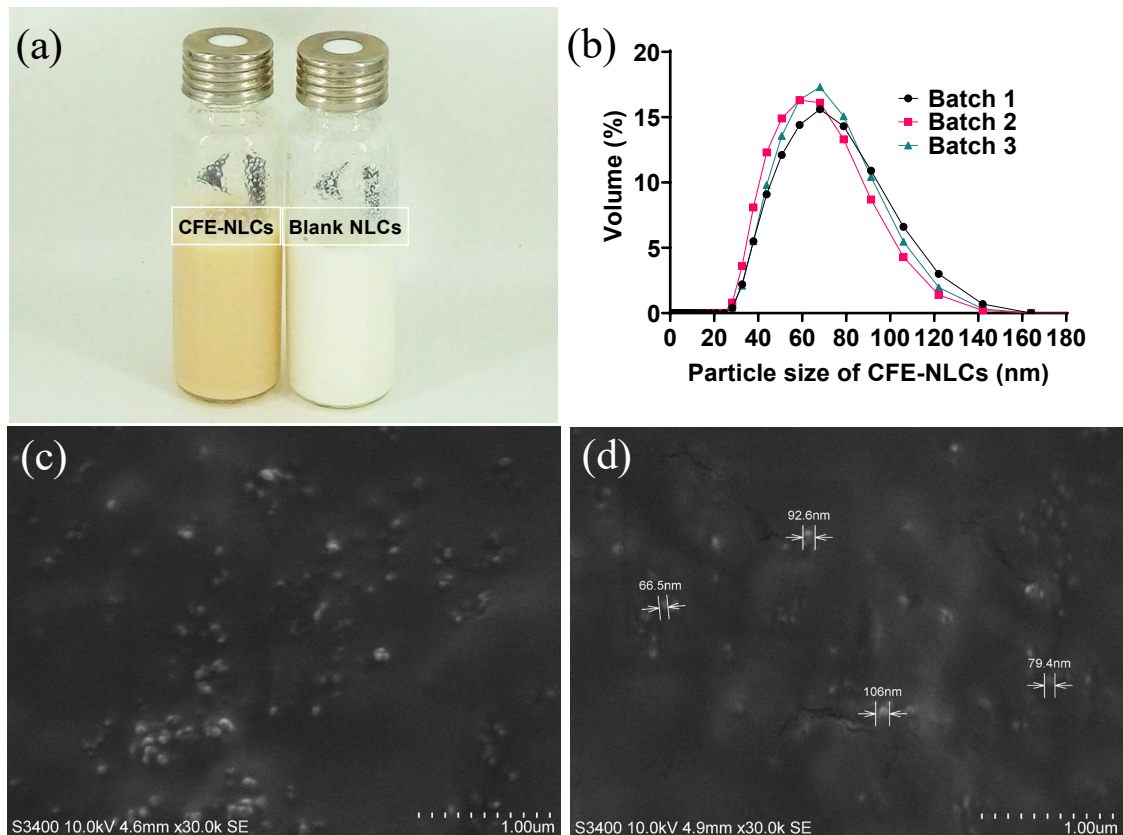


Figure S6. Physical properties of the optimal CFE-NLCs and blank NLC aqueous dispersions prepared under optimized conditions: (a) physical appearance; (b) hydrodynamic diameter of CFE-NLCs prepared from 3 different batches; (c) SEM image of CFE-NLCs; and (d) SEM image of blank NLCs.

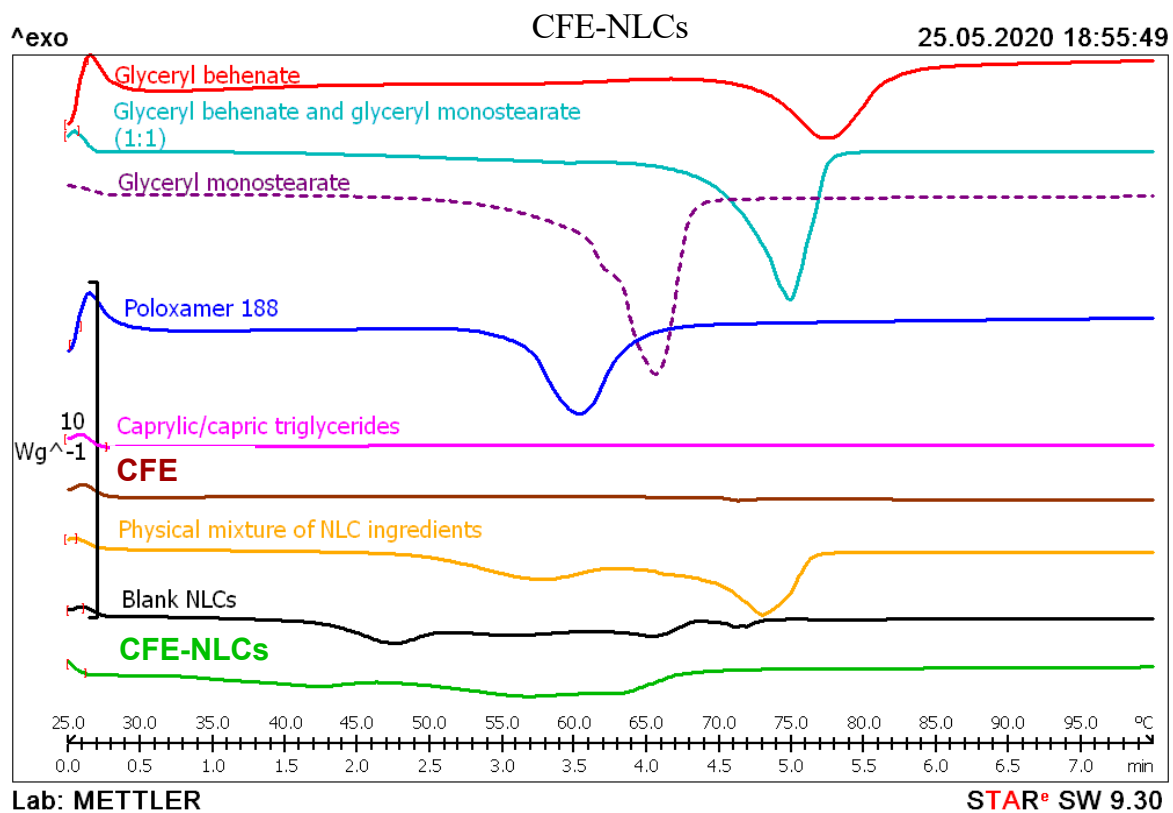


Figure S7. DSC thermograms of CFE-NLCs, blank NLCs and their components.

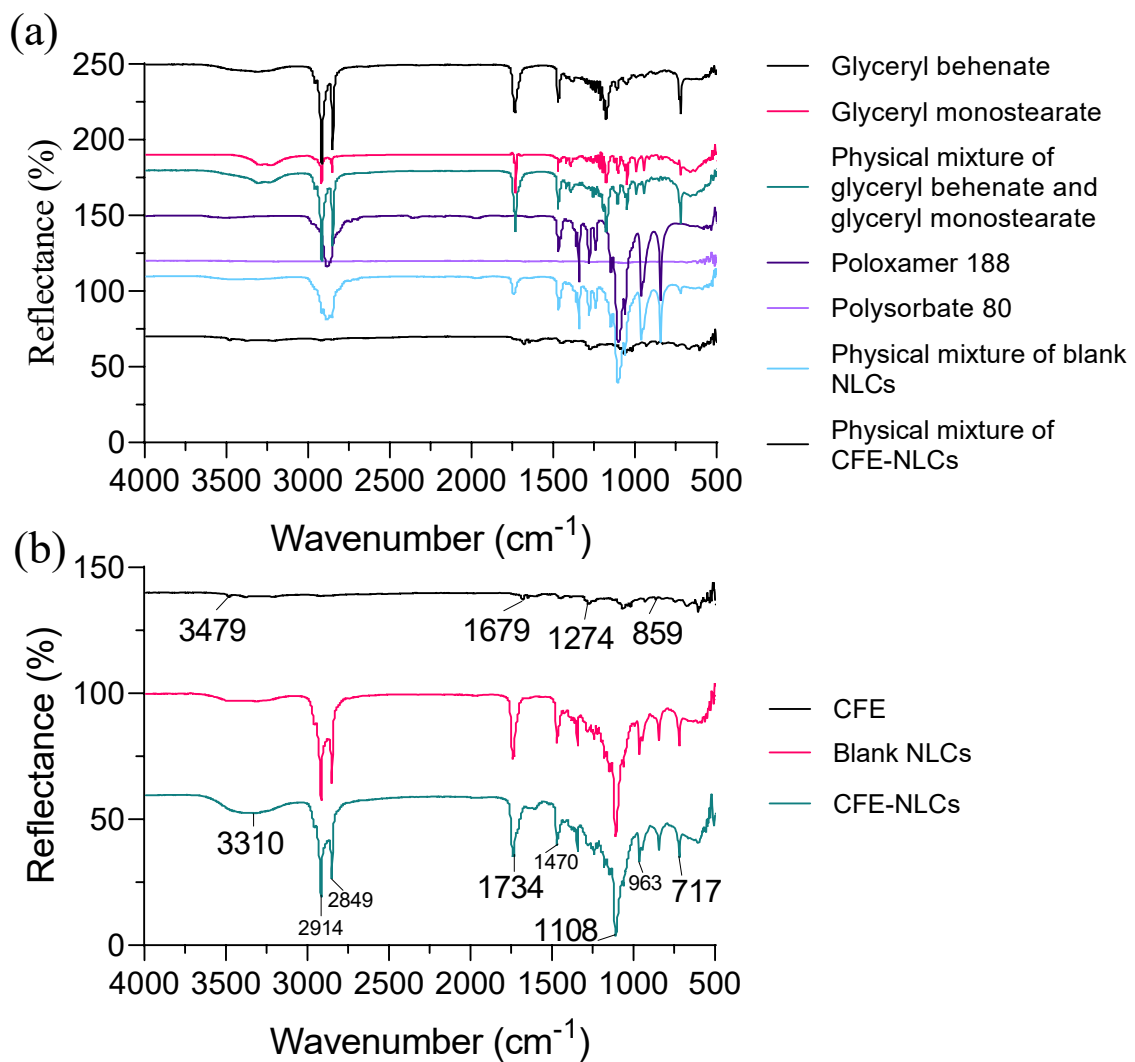


Figure S8. Plots showing ATR-FTIR spectra of (a) NLC compositions and (b) CFE, CFE-NLCs and blank NLCs.

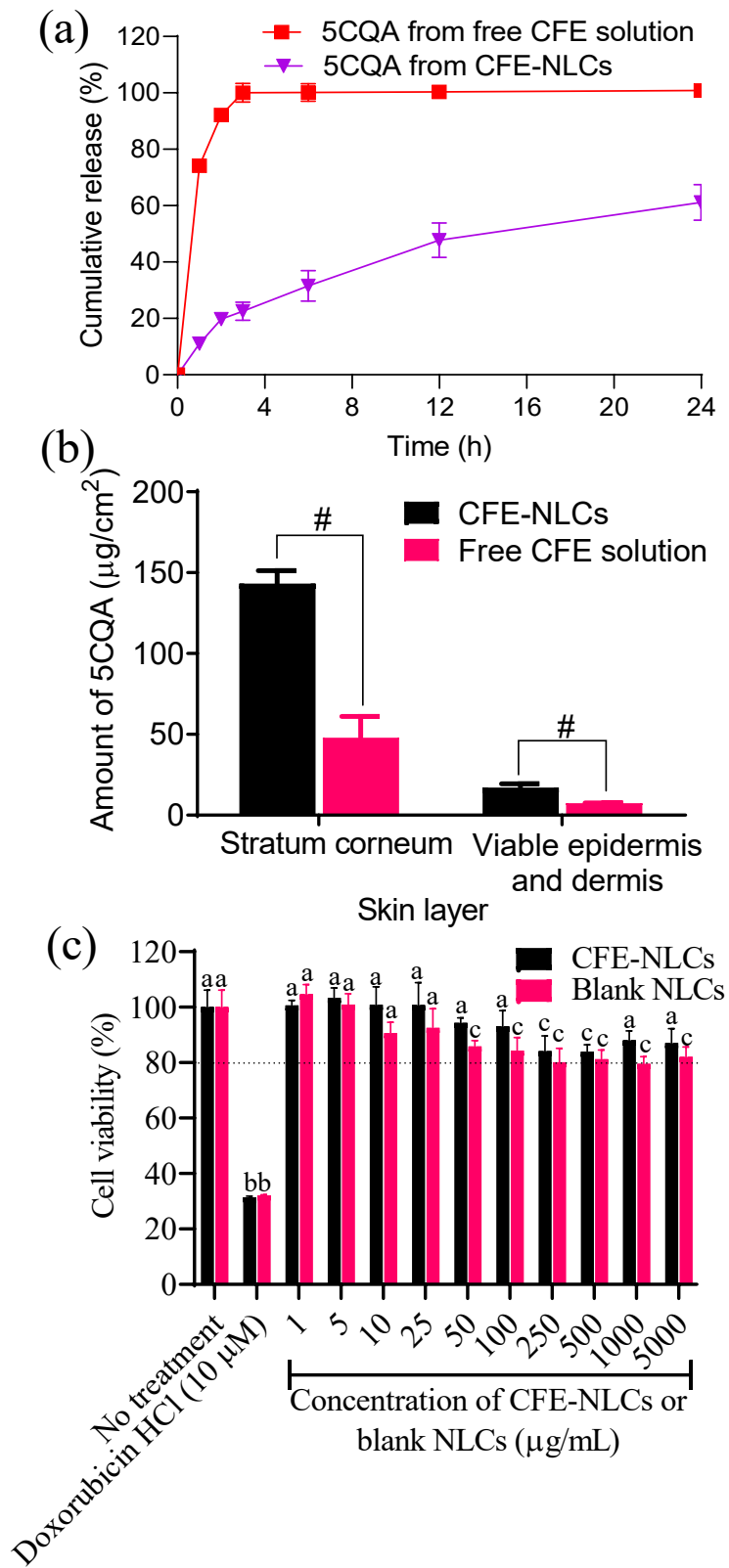


Figure S9. (a) In vitro release of total polyphenols and 5CQA. (b) In vitro permeation studies showing the amount of 5CQA retained in the stratum corneum and the viable epidermis and epidermis layers after 24 h of incubation ([#] $p < 0.001$, $n = 3$). (c) Cytotoxicity of CFE-NLCs and of a blank NLC dispersion to HDFn cells ($n = 3$).

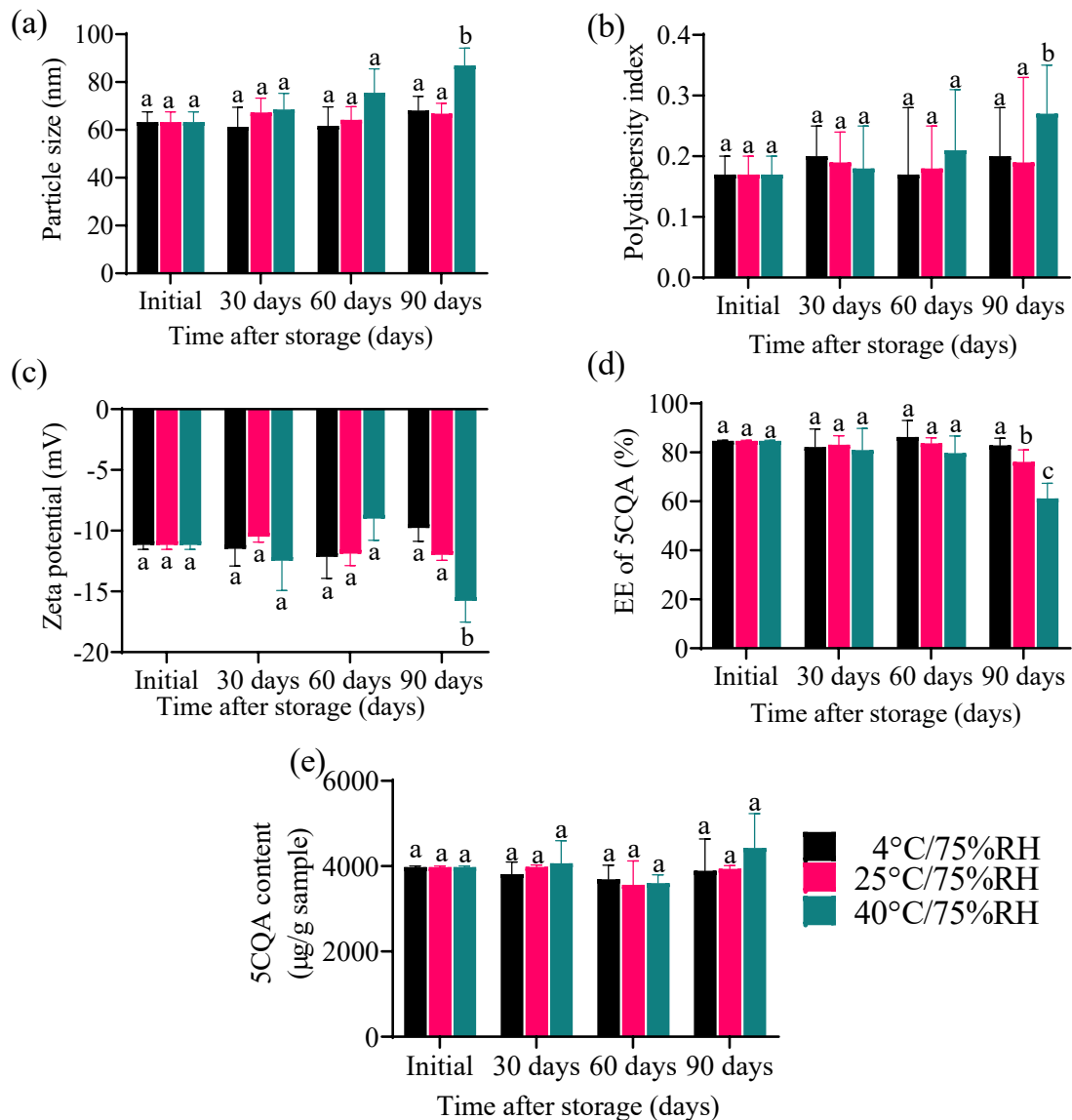


Figure S10. Physicochemical stability of CFE-NLCs and free CFE solution initially and after storage at $4\pm 2^\circ\text{C}$, $25\pm 2^\circ\text{C}$ and $40\pm 2^\circ\text{C}/75\pm 3\%$ relative humidity for 90 days: (a) particle size; (b) PDI; (c) zeta potential; (d) %EE of 5CQA; and (e) content of 5CQA in CFE-NLCs. Values with the same letter above the bar exhibit no significant difference compared with the initial values ($p > 0.05$) ($n = 3$).